EasyChair Preprint

№ 1452

Field-hardened Robotic Autonomy for Subterranean Exploration

Tung Dang, Frank Mascarich, Shehryar Khattak, Huan Nguyen, Nikhil Khedekar, Christos Papachristos and Kostas Alexis

September 3, 2019

Field-hardened Robotic Autonomy for Subterranean Exploration

Tung Dang*, Frank Mascarich*, Shehryar Khattak*, Huan Nguyen, Nikhil Khedekar, Christos Papachristos, and Kostas Alexis

Abstract In this paper a comprehensive approach to enable resilient robotic autonomy in subterranean environments is presented. Emphasizing on the use of aerial robots to explore underground settings such as mines and tunnels, the presented methods address critical challenges related to extreme sensor degradation, path planning in large-scale, multi-branched and geometrically-constrained environments, and reliable operation subject to lack of communications. To facilitate resilience in such conditions, novel methods in multi-modal localization and mapping, as well as graph-based exploration path planning are proposed and combined with custom system design. Through a set of field evaluation activities in real-life subterranean environments we present a "field–hardened" solution that demonstrably enables reliable robotic operation in the hard to access but often crucial underground settings.

Tung Dang
Autonomous Robots Lab, University of Nevada, Reno e-mail: tung.dang@nevada.unr.edu

Frank Mascarich
Autonomous Robots Lab, University of Nevada, Reno e-mail: fmascarich@nevada.unr.edu

Shehryar Khattak
Autonomous Robots Lab, University of Nevada, Reno e-mail: shehryar@nevada.unr.edu

Huan Ngyuen
Autonomous Robots Lab, University of Nevada, Reno e-mail: huann@nevada.unr.edu

Nikhil Khedekar
Autonomous Robots Lab, University of Nevada, Reno e-mail: nikhilvkhedekar@gmail.com

Christos Papachristos
Autonomous Robots Lab, University of Nevada, Reno e-mail: cpapachristos@unr.edu

Kostas Alexis
Autonomous Robots Lab, University of Nevada, Reno e-mail: kalexis@unr.edu

* authors have contributed equally.

1 Introduction

Robotic systems are paving their way to be utilized in an ever–increasing set of applications in both civilian and military domains alike. Aerial robots, for example, are currently utilized in a multitude of surveillance [1], industrial inspection [2], search and rescue [3, 4], and commercial applications [5]. Nevertheless, not every environment is currently rendered possible for robotic entry and autonomous navigation. In this work, we focus on the problem of autonomous exploration and mapping in subterranean settings. Subterranean environments are dull, dirty and dangerous and are characterized by a set of properties that so far have rendered them hard for *autonomous* flying robots. These relate especially to the fact that underground areas are often a) dark, textureless, obscurants-filled and broadly sensing-degraded, b) extremely long, large-scale, narrow and multi-branched, and c) communications-deprived. Despite these major challenges, the benefits of robotic autonomy underground can be very important across application domains. Robots for mine rescue in emergency conditions inside underground mines, inspection of subterranean metropolitan infrastructure (e.g., subways, sewers), exploratory missions within caves and lava tubes in both terrestrial and extraterrestrial environments, are indicative domains of relevant application. Currently, flying drones are used in underground environments with success but their operation is manual thus prohibiting the scalability and versatility of their utilization.

Fig. 1 Instances of autonomous graph-based exploration path planning in subterranean environments. The presented results are based on field tests inside both active and inactive metal mines.

In response to these needs and challenges, this paper presents a holistic work to facilitate resilient robotic autonomy for subterranean exploration. First it outlines a set of contributions on multi-modal sensor fusion for robust localization and mapping with a special focus on thermal vision fusion to penetrate through obscurants such as dust and smoke. Second, it describes a novel approach on exploration path planning in multi-branched and tunnel-like underground environments which is motivated by the observed limitations of previous methods. In addition to the above, it outlines the overall system design. Figure 1 presents an instance of the operation of the presented autonomous aerial robotic scouts for underground settings. This paper presents a comprehensive overview of the aforementioned contributions.

The remainder of this paper is structured as follows. Section 2 overviews the related work. Section 3 outlines the robot design, followed by Section 4 outlining the developed sensing-degraded localization and mapping approach. Section 5 presents the exploration path planner for subterranean environments, while Section 6 details field evaluation studies. Finally, conclusions are drawn in Section 7.

2 Related Work

A niche community has been developed that investigates solutions to the problem of subterranean exploration. The worksin [6, 7] present methods for topological exploration of subterranean environments based on edge exploration and the detection of intersections. It has been verified on ground platforms with the Groundhog system presenting pioneering levels of exploration capacity. The works in [8–13] present contributions in autonomous localization in underground environments. From a systems perspective, the works in [14–19] overview technological innovations in aerial, ground and submersible subterranean robotics. With the domain getting advanced traction largely due to the ongoing DARPA Subterranean Challenge, in this paper we present a holistic contribution on the methods and systems for subterranean autonomy capable of a) sensing-degraded localization and mapping, b) exploration path planning in multi-branched and large-scale tunnel-like settings, and c) robust and resilient operation with absolutely no human teleoperation. Our work is tailored to the subterranean domain but at the same time broadly focused on the two core problems of GPS-denied localization subject to visually-degraded environments and efficient path planning in very narrow and confined long spaces.

3 Subterranean Aerial Scouts

The presented work is based on the development of the subterranean "Aerial Scouts". The intended mission profile of the scouts relates to two types of activities, namely a) autonomous exploration, rapid response and mine-rescue, as well as b) comprehensive inspection, precise mapping and characterization. The robots are designed to be operational in both portal underground mines and mines with hoist-based sub-level access despite the presence of relatively narrow drifts (e.g. $<$ 2m in width). A DJI Matrice 100 quadrotor was used as the platform basis. An Intel NUC Core-i7 computer (NUC7i7BNH) was carried on-board the robot. The integrated sensing solutions were of two different types. The first consists of a) a LiDAR (Velodyne PuckLITE), b) a visible-light camera (FLIR Blackfly), and c) a temperature-calibrated Inertial Measurement Unit (VectorNav VN-100). The second solution replaces the visible-light camera with a 640×512 resolution LWIR thermal vision system running at 60FPS (FLIR Boson). The camera-to-IMU extrinsics were identified based on the work in [20]. The intrinsic calibration parameters of the thermal camera were calculated using our custom designed thermal checkerboard pattern [21]. The camera-to-LiDAR calibration was derived based on an implementation of the work in [22]. For the purposes of control, the robot utilizes the low–level attitude control of the DJI system and implements a Linear Model Predictive Control (MPC) as in [23]. Finally, the aerial scouts further ferry a Dual Band WiFi communication system onboard which is combined with a ground station that integrates a high-gain (19 dBi) Dual Polarized Flat Panel Antenna. However, despite the amplified signal, a reliable high–bandwidth connection is not possible,

especially after turns, thus rendering resilient communications-denied autonomy a necessity. A block-diagram of the basic functionalities of the Aerial Scouts is shown in Figure 2.

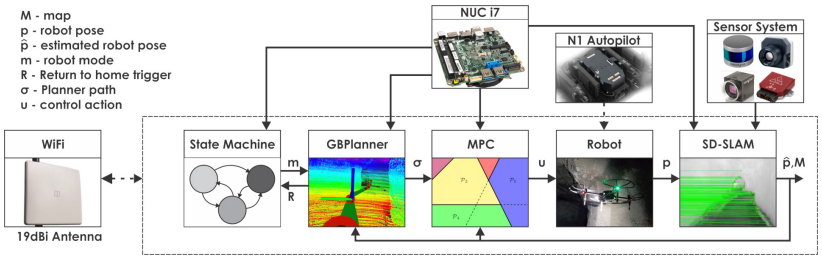

Fig. 2 Block-diagram view of the core functional modules of the aerial scouts. A state machine is responsible to enable the correct mode of robot operation, namely a) auto take-off, b) autonomous exploration, c) return-to-home, and d) auto landing.

4 Sensing-degraded Localization And Mapping

Subterranean settings pose major challenges for robotic perception. Environments such as underground mines, subway tunnels, cave networks or lava tubes are often sensing-degraded including the fact that they are often a) dark, b) textureless, c) obscurants-filled (e.g. dust, smoke), d) particularly narrow, and e) occasionally self-similar. These challenges push the limits of GPS-denied robotic localization and mapping and call for solutions that overcome such difficulties. Traditional vision-based or visual-inertial odometry approaches are bound to fail in conditions of extreme visual degradation which can be the case in a dust–filled underground mine or a subway network filled with smoke in case of an accident. Similarly, methodologies that rely only on LiDAR can face extreme difficulties in self-similar environments [24]. In response to these facts it is identified that methods relying on a single exteroceptive modality are likely to present failure, and thus a multi-modal methodology is proposed. Simultaneously, the case of thermal vision-inertial sensing fusion is explicitly addressed as it provides a solution for most cases of obscurants-filled environments. Using LongWave InfraRed (LWIR) vision, common obscurants such as dust or fog are seamlessly penetrated.

4.1 Multi-Modal Localization And Mapping

Towards resilient and resourceful localization in sensing-degraded underground environments, the fusion of LiDAR, vision, thermal camera and inertial sensing is

proposed. As a first solution, a loosely-coupled approach is considered with a robot implementing odometry solutions based on the above sensing modalities or a subset of them. More specifically, in the framework of our work we specifically consider the case of LiDAR-vision-IMU fusion or LiDAR-thermal-IMU fusion. LiDAR and IMU data are fused based on the LiDAR Odometry And Mapping (LOAM) algorithm proposed in [25] thus leading to a generally reliable odometry estimation and accurate map that can, however, be ill–conditioned in cases of self-similar geometries or the presence of very dense obscurants. Visual-inertial or thermal-inertial fusion is achieved either through the use of the RObust Visual Inertial Odometry (ROVIO) framework [26] or through our recently proposed Keyframe-based Thermal-Inertial Odometry (KTIO) method [27] (specifically for thermal vision). The individual odometry estimates are then fused on a cascade Extended Kalman Filter based on the Multi Sensor Fusion (MSF) framework [28] with the LiDAR odometry considered to have a fixed- and rather small-valued covariance update matrix, unless when ill–conditioning is detected as per the work in [24], thus allowing the camera-based solution to dominate. This loosely-coupled approach is outlined in Figure 3 and although relatively straightforward it allows resourcefulness that would otherwise be impossible. A new approach on tight fusion is briefly outlined in Section 7.

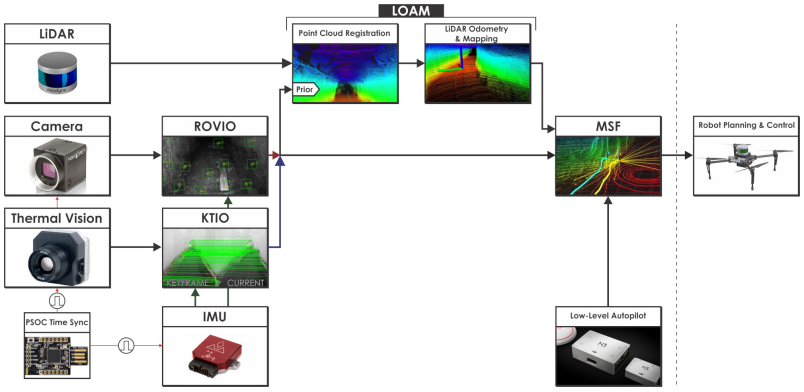

Fig. 3 Loosely-coupled multi-modal fusion for odometry estimation. LiDAR is used for full odometry and mapping and associated with fixed covariance which is only inflated when ill-conditioning is detected due to geometric self-similarity. Camera-IMU odometry estimation takes place simultaneously while the two classes of updates are merged in an Extended Kalman Filter (MSF).

4.2 Thermal-inertial Odometry

Longwave infrared thermal vision (e.g., 7.5 - 13.5μm) allows to penetrate a variety of solutions such as dust or fog, thus offering a viable alternative to traditional camera-based localization in degraded obscurants-filled settings. Thermal camera

systems typically provide a radiometric image with more than 8–bit resolution (e.g. 14-bit in the case of the FLIR Tau2 Core). However, most work on the utilization of thermal vision for odometry estimation have rescaled the image such that traditional vision-based odometry schemes (made for grayscale 8-bit frames) can be directly applied. This approach however has major limitations as it a) leads to information loss and does not allow the detection of thermal gradients on the full-resolution image, and b) relies on histogram-equalization techniques, most commonly implemented as Automatic Gain Control (AGC) schemes, to rescale the image in a local thermal region which, however, leads to extreme changes in intensity when the scene suddenly involves much colder or much warmer bodies. Simultaneously, heuristic efforts to fix the rescaling region also leads to major information loss and assumes a priori knowledge of the temperature and emmissivity aspects of the scene.

In response to these limitations, we recently proposed the Keyframe-based direct Thermal-Inertial Odometry (KTIO) which a) works directly on 16–bit radiometric data, b) operates without relying on traditional feature detection and description methods made for 8–bit images and thus remains generalizable across environments, and c) employs a joint-optimization architecture in which IMU feeds are incorporated as constraints. Relying on a keyframe–based approach also offers robustness against periods of data loss which in fact happen during the Flat Field Correction (FFC) operation of thermal cameras that commonly last for 500ms. More specifically, KTIO relies on a 2–stage architecture that can be divided into a front–end component and a back–end component. This bifurcation allows us to run our odometry estimation framework in a multi–threaded manner on modern processors. The key responsibility of the front–end component is to perform an alignment between an incoming image to previous images in the camera coordinate frame $(\mathcal{C})$ based on the minimization of radiometric error and to initialize 3D landmarks in the world coordinate frame $(\mathcal{W})$. Given a set of 3D landmarks, the key responsibility of the back–end component is to estimate odometry by jointly minimizing the re–projection errors in landmark positions and the intra–frame inertial measurement errors over a sliding window. An overview of the approach is shown in Figure 4. As shown, the front-end component performs four major operations, namely a) image alignment, b) point initialization, c) point refinement, and d) landmark initialization and pruning. Thus, it replaces all tasks usually associated with feature detection, matching and pruning in traditional feature-based approaches while the full operation takes place in full 16-bit resolution. Given a set of 3D landmarks and inertial measurements between image frames, the back-end is then responsible for full pose estimation by solving a non-linear optimization problem that minimizes the re-projection errors of the observed landmarks, while respecting inertial constraints. Thus, pose estimation is cast as a joint thermal-inertial problem. Full formulation details of KTIO can be found at [27]. Effectively, this method allows robust estimation of the robot state, IMU bias and landmark locations, despite the presence of obscurants. Its output is then fused into the cascade Extended Kalman Filter (MSF).

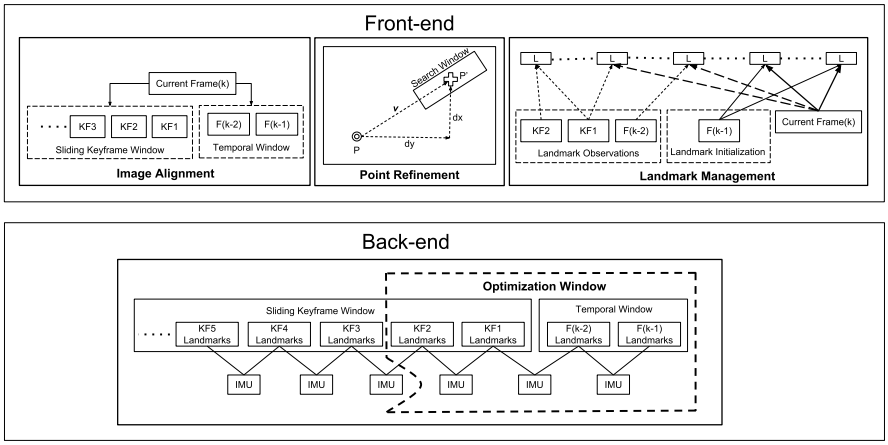

Fig. 4 Overview of KTIO. The front–end component is responsible for aligning the incoming image to the last two received images and to the last two key–frames. If alignment of the current image with a past images or key–frames is successful, location of points in the current image are refined to determine their localization quality. Points with good localization quality are then triangulated to either add observations to previously observed landmarks or initialize new landmarks. Using the initialized landmarks the back–end jointly optimizes the landmark re–projection and intra–frame inertial measurement errors in a sliding window approach to estimate the robot pose.

5 Exploration Path Planning Underground

Subterranean settings are often comprised of very large-scale narrow tunnel networks with multiple branching points and long geometrically-constrained drifts. Examples include those of underground mines, metropolitan subway infrastructure, and cave networks. In response to these facts, the proposed Graph-Based exploration path Planner (GBPlanner) provides fast and efficient solutions for volumetric exploration despite the large-scale and geometrically-constrained character of such environments, while simultaneously offering a) safe return-to-home functionality, and b) solution resourcefulness when the exploration process reaches a dead-end (e.g. a mine heading). The exploration planning problem is defined as follows:

Problem 1 (Exploration Problem). Given an occupancy map $\mathbb{M}$, find a collision-free path $\sigma^* = \{\xi_i\}$ ($\xi_i = [x_i, y_i, z_i, \psi_i]^T$ being the flat rigid body configuration) to guide the robot towards unmapped areas and ensure the exploration of the perceivable volume V_E within the total and initially unknown volume V. Under the assumption of a depth sensor $\mathbb{S}$ with maximum effective range $d_{\max}$ and perception that stops at surfaces, the perceivable volume is defined as $V_E = V \setminus V_{res}$, where V_{res} is the residual volume for which no robot configuration exists to map it.

The general operation of the GBPlanner is depicted in Figure 5. As shown, the planner is organized in a local- and a global-planning stage architecture.

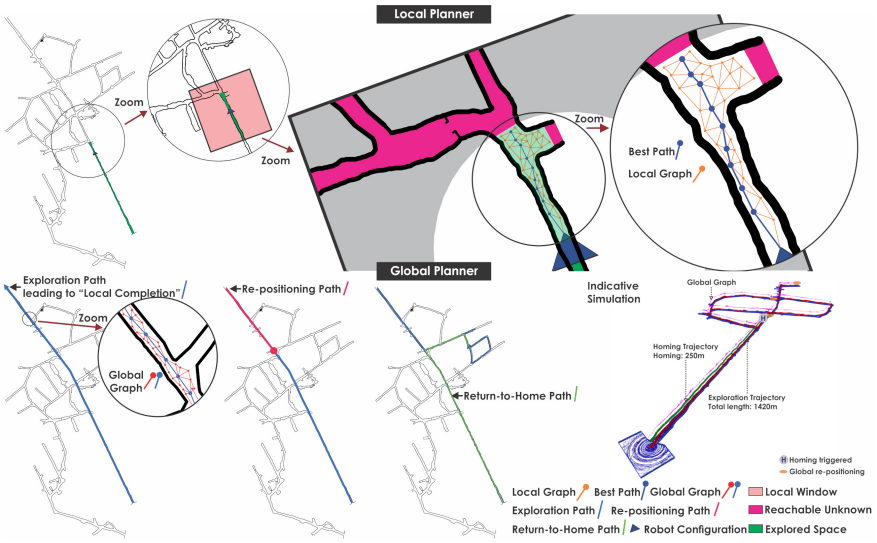

Fig. 5 Key steps of the proposed planner. The local planner operates within a window around the current robot location, samples a graph and identifies the path that maximizes the exploration gain. The global planner offers two functionalities, namely a) re-position to the frontier of the exploration space when a "dead-end" is reached, and b) return-to-home. For both tasks, the global planner utilizes a graph incrementally built during the robot operation thus saving the time that it would take to sample a new graph from scratch.

5.1 Local Planner

Most commonly, the GBPlanner operates with the local planner engaged. The local planner operates within a local map subset $\mathbb{M}_L \subset \mathbb{M}$ centered around the current robot configuration ξ_0. Operating in a local window allows to perform a comprehensive search while remaining computationally lightweight. The local planner operates by first sampling an undirected graph $\mathbb{G}_L$ based on the Rapidly-exploring Random Graph (RRG) algorithm [29] starting from ξ_0 as the root. Subsequently, Dijkstra's algorithm is used to find all shortest paths $\{\sigma_i\}$ from ξ_0 to all sampled vertices. Then, every such path σ_i, $i = 1...n$ is evaluated with respect to the exploration gain primarily based on calculating the new volume to be explored:

$$\textbf{ExplorationGain}(\sigma_i) = e^{-\gamma_S \mathcal{S}(\sigma_i, \sigma_{exp})} \sum_{j=1}^{m_i} \textbf{VolumetricGain}(v_j^i) e^{-\gamma_D \mathcal{D}(v_1^i, v_j^i)} \tag{1}$$

where m_i is the number of vertices in σ_i, $\mathcal{S}(\sigma_i, \sigma_{exp})$, $\mathcal{D}(v_1^i, v_j^i)$ are weight functions with tunable factors $\gamma_S, \gamma_D > 0$, and $\mathcal{D}(v_1^i, v_j^i)$ is the cumulative Euclidean distance from a vertex v_j^i to the root v_1^i along the path σ_i. This aims to penalize longer paths in order to favor a higher exploration rate. Moreover, $\mathcal{S}(\sigma_i, \sigma_{exp})$ is a similarity distance metric between the planned path as compared to a pseudo–

straight path σ_{exp} with the same length along the current exploration direction. This decay factor is essential to prevent the robot from a sudden change in its "exploration direction" which might happen when the robot enters an intersection area with multiple branches or muckbays and the planner proposes small back-and-forth paths between them to chase higher rewards based on the local volumetric calculation. If the branch is large and thus gain is significant, then this term is tuned to play an insignificant role. The exploration direction is simply estimated using a low-pass filter over a time window of robot positions. Given this exploring direction vector, denoted as ϕ_{exp}, we then generate a pseudo–straight path σ_{exp} using the same length with σ_i. Subsequently, the Dynamic Time Warping method (DTW) [30] is utilized to compute the similarity distance metric. Given the weighted calculation of the gain, and the derivation of Dijkstra solutions, the Dijkstra path $\sigma_{L,best}$ that maximizes for exploration gain is selected and conducted by the robot, while the whole procedure is then iteratively repeated. It is noted that when the local planner cannot report a path that exceeds an exploration gain above a small threshold $g_\varepsilon > 0$, then the global planner is engaged.

5.2 Global Planner

The global planner contributes two key roles in the GBPlanner exploratory behavior, namely that of a) deriving a safe return-to-home functionality, and b) identification of paths that re-position the robot at the edge of the exploration space when the local planner has followed a high–gain route that, however, has eventually led to a dead-end. To implement its functionality, the global planner utilizes the incrementally sampled local graphs $\{\mathbb{G}_L\}$ alongside the actual robot odometry to build the global graph $\mathbb{G}_G$. At every iteration, $\mathbb{G}_G$ is utilized to identify a return-to-home path σ_{RH} after a re-sampling step has taken place to introduce more edges and thus improve the ability to find shorter paths especially when the robot has passed more than once from the same region. This homing path is engaged when the robot endurance is such that continuation of the exploration mission and return to home is not possible. Simultaneously, $\mathbb{G}_G$ is also utilized when the local planner reports inability to derive a path of significant exploration gain and while sufficient battery time is available. In such a case, the exploration gain associated with all vertices of $\mathbb{G}_G$ is calculated thus allowing to identify the parts visited before that are at the edge of the exploration space. A route σ_{RE} is then calculated that repositions the robot to the best vertex at the edge of the known space. Subsequently, the local planner is re-engaged.

6 Field Evaluation for Resilient Autonomy

In order to systematically evaluate the proposed subterranean exploration autonomy solution, a set of activities in real underground mines took place. In this work we present three results from underground metal mines in the U.S. and in Switzerland.

As a first result, we present the autonomous exploration of a subset of the production level of an active and modern underground gold mine in Nevada. The production level is characterized by a) long yet reasonably wide drifts and frequent presence of headings or muckbays for equipment storage, b) intense sensor degradation due to dense dust amplified by the flying robot-generated turbulence, and c) dark and not always texture-rich environments. The autonomous mission is organized in three phases, namely: a) automatic take-off, b) engaging the GBPlanner and performing autonomous exploration up to the point that the local planner reports completion (inability to find a further path to explore), c) automated landing. The emphasis in this mission is on the behavior of the local step of the planner. Figure 6 presents instances and the full result of the execution of this mission.

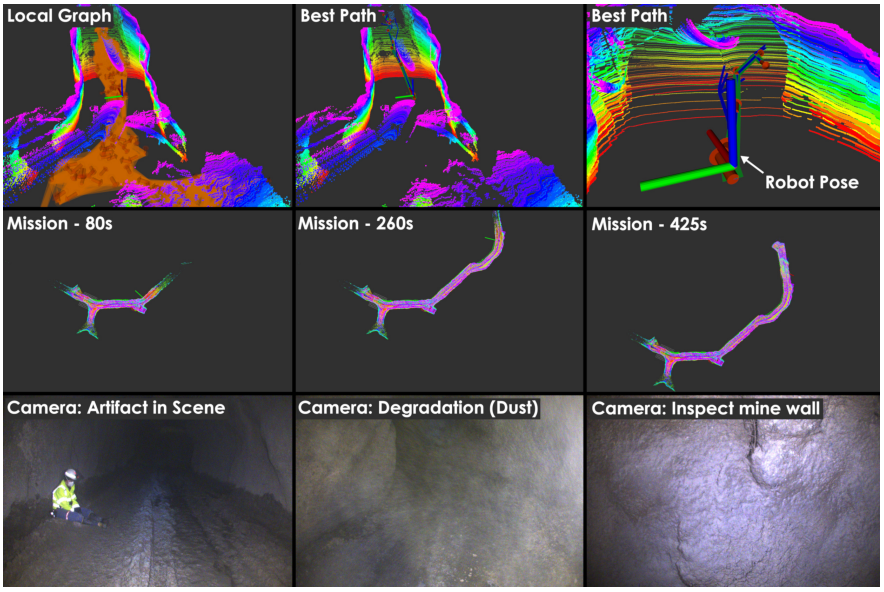

Fig. 6 Autonomous exploration of the production level of an underground gold mine. The first row presents both the local graph and the selected path, while instances of the overall map reconstruction are shown in the second row. Finally, images from the onboard camera, including a case of dust-based degradation, are shown in the last row. A video of this mission can be found at `https://youtu.be/_96vVchOsvk`

The second result relates to a deployment of the presented robotic systems at the "Lucerne" underground mine at Northern Nevada. This is a portal mine which allowed the robot deployment to take place from above ground and the systems were

tasked to autonomously access and explore the mine. In this deployment, first a robot equipped with LiDAR, visible-light camera and IMU conducted two sequential missions to autonomously explore and map the mine. With the support of three AprilTags and the method in [31] it became possible to reference robot data from multiple missions against a common reference frame. Figure 7 depicts the reconstructed point clouds from two missions of the robot. As shown, based on the external frame alignment achieved with the support of the AprilTags, it became possible to have aligned point clouds from two different missions. This also facilitates the ability to report coordinates against an external frame, a fact particularly important when it comes to providing intelligence to teams that need to plan certain actions (e.g. in the case of mine or cave rescue). In addition, this result is also an indirect verification of the quality of the localization and mapping solution as two different runs led to close-to-identical maps. Finally, in these experiments a robot that also integrates thermal sensing, alongside LiDAR and IMU, was also utilized. Therefore, it became possible to evaluate the performance of our proposed Keyframe-based Thermal-Inertial Odometry (KTIO). Figure 8 presents relevant odometry comparison. As shown the error between the two solutions is small.

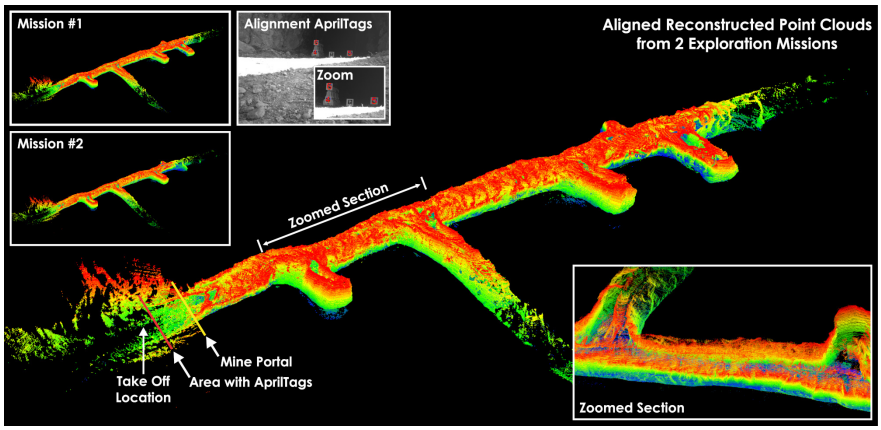

Fig. 7 Simultaneous representation of two reconstructions of the "Lucerne" underground mine achieved through two sequential autonomous exploration missions and the use of AprilTags positioned at the mine portal in order to facilitate a common reference frame between the robots. This also facilitates the ability to report coordinates against an external frame (e.g. georeferencing) as it would be required for example to schedule rescue activities in the case of a mine accident.

Lastly, a result in which the robot is tasked to explore an unknown area, while eventually returning to the home location is presented. In this mission, the GBPlanner tracks the remaining battery life of the system in order to engage the global planning stage such that it can derive a path to safely come back to its initial take-off location. This field test took place at the Gonzen Mine, an abandoned iron mine in Sargans, Switzerland. As opposed to the previous mine environments, Gonzen presents the challenge of very narrow drifts and corridors, often less than 2m wide,

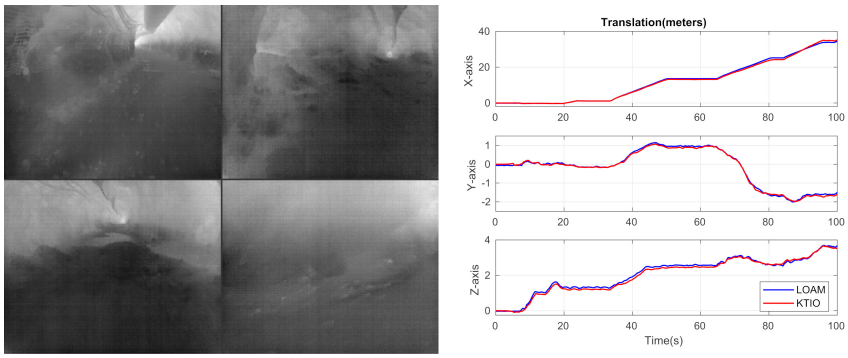

Fig. 8 Right: Odometry comparison between the Keyframe-based Thermal-Inertial Odometry (KTIO) and LiDAR Odometry And Mapping (LOAM). The $[x,\ y,\ z]$ RMSE values are $[0.52,\ 0.06,\ 0.09]$m respectively. Left: Indicative, rescaled, thermal camera frames from the mine.

alongside sharp turns. Figure 9 presents a short exploratory mission followed by an autonomously triggered return-to-home path.

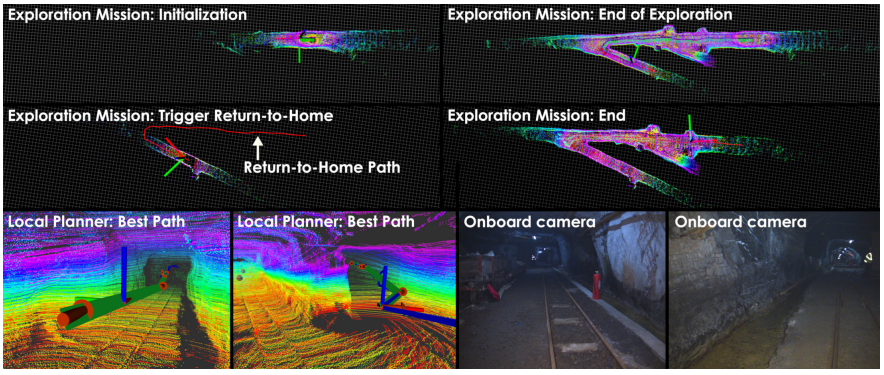

Fig. 9 Exploration inside the Gonzen iron mine in Switzerland and safe autonomously triggered return-to-home mission. The first row presents the initial and final robot pose in the exploratory phase, while the second row presents the return-to-home path followed by the instance of the robot arriving at its initial take–off location. Finally, the last row presents best paths of the local planner, alongside indicative camera frames from the onboard color vision sensor. A video of this mission can be found at `https://youtu.be/982iwe8qZGk`

7 Conclusions

This paper detailed a comprehensive solution for autonomous subterranean exploration using aerial robots. To achieve this challenging task, contributions across the

domains of sensing-degraded localization, as well as informative path planning took place combined with system development and optimization. Extensive field testing in actual subterranean environments, specifically inside underground mines, allowed to evaluate the system and optimize its functional loops. Future research will emphasize on two prioritized directions, namely a) a common multi-modal localization and mapping based on factor graph optimization, and b) extension of the planning framework for ground systems by accounting for example for traversability analysis over rough terrain.

Acknowledgement

This material is based upon work supported by the Defense Advanced Research Projects Agency (DARPA) under Agreement No. HR00111820045. The presented content and ideas are solely those of the authors.

References

1. B. Grocholsky, J. Keller, V. Kumar, and G. Pappas, "Cooperative air and ground surveillance," *IEEE Robotics & Automation Magazine*, vol. 13, no. 3, pp. 16–25, 2006.
2. A. Bircher, K. Alexis, M. Burri, P. Oettershagen, S. Omari, T. Mantel and R. Siegwart, "Structural inspection path planning via iterative viewpoint resampling with application to aerial robotics," in *IEEE International Conference on Robotics and Automation (ICRA)*, pp. 6423–6430, May 2015.
3. H. Balta, J. Bedkowski, S. Govindaraj, K. Majek, P. Musialik, D. Serrano, K. Alexis, R. Siegwart, and G. De Cubber, "Integrated data management for a fleet of search-and-rescue robots," *Journal of Field Robotics*, vol. 34, no. 3, pp. 539–582, 2017.
4. T. Tomic, K. Schmid, P. Lutz, A. Domel, M. Kassecker, E. Mair, I. L. Grixa, F. Ruess, M. Suppa, and D. Burschka, "Toward a fully autonomous uav: Research platform for indoor and outdoor urban search and rescue," *IEEE robotics & automation magazine*, 2012.
5. B. Rao, A. G. Gopi, and R. Maione, "The societal impact of commercial drones," *Technology in Society*, vol. 45, pp. 83–90, 2016.
6. D. Silver, D. Ferguson, A. Morris, and S. Thayer, "Topological exploration of subterranean environments," *Journal of Field Robotics*, vol. 23, no. 6-7, pp. 395–415, 2006.
7. C. Baker, A. Morris, D. Ferguson, S. Thayer, C. Whittaker, Z. Omohundro, C. Reverte, W. Whittaker, D. Hahnel, and S. Thrun, "A campaign in autonomous mine mapping," in *IEEE International Conference on Robotics and Automation, 2004. Proceedings (ICRA)*, 2004.
8. P. Debanne, J.-V. Herve, and P. Cohen, "Global self-localization of a robot in underground mines," in *1997 IEEE International Conference on Systems, Man, and Cybernetics. Computational Cybernetics and Simulation*, vol. 5, pp. 4400–4405, IEEE, 1997.
9. C. Kanellakis and G. Nikolakopoulos, "Evaluation of visual localization systems in underground mining," in *2016 24th Mediterranean Conference on Control and Automation (MED)*, pp. 539–544, June 2016.
10. J. M. Roberts, E. S. Duff, and P. I. Corke, "Reactive navigation and opportunistic localization for autonomous underground mining vehicles," *Information Sciences*, 2002.
11. D. Wu, Y. Meng, K. Zhan, and F. Ma, "A lidar slam based on point-line features for underground mining vehicle," in *2018 Chinese Automation Congress (CAC)*, IEEE, 2018.

12. F. Zeng, A. Jacobson, D. Smith, N. Boswell, T. Peynot, and M. Milford, "I2-s2: Intra-image-seqslam for more accurate vision-based localisation in underground mines," in *Australasian Conference on Robotics and Automation 2018*, December 2018.
13. F. Zeng, A. Jacobson, D. Smith, N. Boswell, T. Peynot, and M. Milford, "Lookup: Vision-only real-time precise underground localisation for autonomous mining vehicles," *arXiv preprint arXiv:1903.08313*, 2019.
14. A. Morris, D. Ferguson, Z. Omohundro, D. Bradley, D. Silver, C. Baker, S. Thayer, C. Whittaker, and W. Whittaker, "Recent developments in subterranean robotics," *Journal of Field Robotics*, vol. 23, no. 1, pp. 35–57, 2006.
15. P. Novák, J. Babjak, T. Kot, P. Olivka, and W. Moczulski, "Exploration mobile robot for coal mines," in *International Workshop on Modelling and Simulation for Autonomous Systems*, pp. 209–215, Springer, 2015.
16. A. Martins, J. Almeida, C. Almeida, A. Dias, N. Dias, J. Aaltonen, A. Heininen, K. T. Koskinen, C. Rossi, S. Dominguez, *et al.*, "Ux 1 system design-a robotic system for underwater mining exploration," in *2018 IEEE/RSJ International Conference on Intelligent Robots and Systems (IROS)*, pp. 1494–1500, IEEE, 2018.
17. A. H. Reddy, B. Kalyan, and C. S. Murthy, "Mine rescue robot system–a review," *Procedia Earth and Planetary Science*, vol. 11, pp. 457–462, 2015.
18. S. Buerger and J. R. Salton, "Autonomous unmanned systems technologies to support subterranean operations.," tech. rep., Sandia National Lab, Albuquerque, NM, USA, 2018.
19. F. Mascarich, S. Khattak, C. Papachristos, and K. Alexis, "A multi-modal mapping unit for autonomous exploration and mapping of underground tunnels," in *2018 IEEE Aerospace Conference*, pp. 1–7, IEEE, 2018.
20. P. Furgale, J. Rehder, and R. Siegwart, "Unified temporal and spatial calibration for multi-sensor systems," in *2013 IEEE/RSJ International Conference on Intelligent Robots and Systems*, pp. 1280–1286, IEEE, 2013.
21. C. Papachristos, F. Mascarich, and K. Alexis, "Thermal-inertial localization for autonomous navigation of aerial robots through obscurants," in *2018 International Conference on Unmanned Aircraft Systems (ICUAS)*, pp. 394–399, June 2018.
22. L. Zhou, Z. Li, and M. Kaess, "Automatic extrinsic calibration of a camera and a 3d lidar using line and plane correspondences," in *2018 IEEE/RSJ International Conference on Intelligent Robots and Systems (IROS)*, pp. 5562–5569, IEEE, 2018.
23. M. Kamel, T. Stastny, K. Alexis, and R. Siegwart, *Model Predictive Control for Trajectory Tracking of Unmanned Aerial Vehicles Using Robot Operating System*, pp. 3–39. Cham: Springer International Publishing, 2017.
24. J. Zhang, M. Kaess, and S. Singh, "On degeneracy of optimization-based state estimation problems," in *2016 IEEE International Conference on Robotics and Automation (ICRA)*, pp. 809–816, IEEE, 2016.
25. J. Zhang and S. Singh, "Loam: Lidar odometry and mapping in real-time.," in *Robotics: Science and Systems*, vol. 2, p. 9, 2014.
26. M. Bloesch, S. Omari, M. Hutter, and R. Siegwart, "Robust visual inertial odometry using a direct ekf-based approach," in *Intelligent Robots and Systems (IROS), 2015 IEEE/RSJ International Conference on*, pp. 298–304, IEEE, 2015.
27. S. Khattak, C. Papachristos, and K. Alexis, "Keyframe-based direct thermal–inertial odometry," in *IEEE International Conference on Robotics and Automation (ICRA)*, May 2019.
28. S. Lynen, M. W. Achtelik, S. Weiss, M. Chli, and R. Siegwart, "A robust and modular multi-sensor fusion approach applied to mav navigation," in *2013 IEEE/RSJ international conference on intelligent robots and systems*, pp. 3923–3929, IEEE, 2013.
29. S. Karaman and E. Frazzoli, "Sampling-based motion planning with deterministic μ-calculus specifications," in *Proceedings of the 48h IEEE Conference on Decision and Control (CDC) held jointly with 2009 28th Chinese Control Conference*, pp. 2222–2229, IEEE, 2009.
30. A. G. Bachrach, *Trajectory bundle estimation For perception-driven planning*. PhD thesis, Massachusetts Institute of Technology, 2013.
31. J. Wang and E. Olson, "AprilTag 2: Efficient and robust fiducial detection," in *2016 IEEE/RSJ International Conference on Intelligent Robots and Systems (IROS)*, IEEE, oct 2016.